

Assessment of two MPPT algorithms for a standalone photovoltaic system with variable weather condition

Claude Bertin Nzoundja Fapi^{1,2*}, Abderrezak Badji^{2,3}, Hyacinthe Tchakounte¹,
Gerald Tsayo Bantio¹, Martin Kamta¹, Patrice Wira²

¹ LESIA Laboratory, ENSAI, University of Ngaoundere, P.O. Box: 455 Ngaoundere, Cameroon

² IRIMAS Laboratory, University of Haute Alsace, 61 Road Albert Camus, F-68093 Mulhouse, France

³ LATAGE Laboratory, Mouloud Mammeri University of Tizi-Ouzou, P.O. Box: 17 RP 15000 Tizi-Ouzou, Algeria

*Corresponding author E-mail: nzoufaclauber@yahoo.fr

Abstract

The electrical power of a photovoltaic (PV) system decreases considerably when weather conditions are variable. In this context, the authors experimentally study on the optimization of the electrical power efficiency of a photovoltaic module using the Fuzzy Logic Control (FLC) method. The main purpose of this work is to extract the maximum energy from a solar panel using the Maximum Power Point Tracker (MPPT) algorithm. This algorithm acts on the DC-DC boost duty cycle of the solar photovoltaic system, depending on weather conditions (temperature and irradiance). To achieve this optimization, firstly, this work presents an experimental implementation of the proposed Fuzzy Logic Control method of a stand-alone photovoltaic system. Secondly, a comparative study between the proposed Fuzzy Logic Control approach and the conventional Perturb and Observe (P&O) MPPT method using Matlab/Simulink is presented. Experimental as far as numerical results based on recorded climatic data from Ngaoundere (in Cameroon) and Mulhouse (in France) cities, show that the FLC approach has several advantages over the conventional P&O MPPT method such as: fast response, robustness, minimal effect of climate fluctuations on the electrical power produced.

Keywords: PV System; Fuzzy Logic Controller; P&O Method; Weather Condition; Numerical Simulation; Experimental Data.

1. Introduction

In this last decade, the demand for high living standards and thus electric energy has been growing progressively. There are many possibilities of energy production such as fossil energy, hydroelectricity, nuclear energy and renewable energy [1]-[4]. Fossil energy as far as nuclear energy is contributing considerably to the pollution of the environment causing enormous socio-economic and human damages, on one hand. In the other hand, hydroelectricity is not available elsewhere [5]-[7]. On this context, renewable energy and in particular photovoltaic (PV) energy systems offer a very competitive solution [8]-[9]. Nevertheless electrical power efficiency of photovoltaic cells remains low. In order to improve the efficiency of the PV panel, it is necessary to optimize the extraction of energy. To achieve such task, the photovoltaic generator must operate at its Maximum Power Point (MPP). This constraint can be done using a Maximum Power Point Tracker (MPPT) controller [10]-[14].

Nowadays, with technological means, there are several methods for MPPT: Fractional Open-Circuit Voltage (FOCV), Fractional Short-Circuits Current (FSCC) [15]-[16], Artificial Neural Network (ANN) technique and the Fuzzy Logic Control (FLC) [17]-[20]. On the other hand, it was also demonstrated in [21] that there are computational techniques to track the maximum power using look-up. Some related tracking methods based on this approach are widely adopted in PV power systems [6]. Among them, the most popular methods are: Perturb and Observe (P&O), Incremental Conductance (INC) [22]-[23] and Hill Climbing (HC). These

techniques are widely applied because of their simplicity. But there is no complete comparison between previous cited techniques and their tracking efficiency under varying weather conditions.

This work shall focus on the investigation of tracking efficiency between P&O and FLC MPPT algorithms in variable weather conditions to see the one which is worthwhile. Some works based on fuzzy logic have already been done in the literature review. In most of them, an extra gain block has been added to the fuzzy system to adjust the output [17], [18]. In this work, the authors develop a particular fuzzy system where a gain block is removed and the duty cycle is calculated directly based on seven rules. The developed algorithm is able to track MPP with appropriate speed, and it shows very good dynamical response with sudden variations in real weather conditions. More importantly, the selection of a suitable converter when implementing a PV-MPPT method is crucial. Recent works have shown that different types of converters have been used for various applications [2], [21], [23]. For this work, a boost topology was selected because it is suitable for high voltage applications. Finally, in Fig. 1 the developed PV module and the MPPT algorithm is coupled to the DC-DC boost to assess the performance of the system.

The purpose of this study is to exploit the photovoltaic panel at the MPP under variable weather conditions to compare P&O and FLC MPPT algorithm.

In Section 2, modeling of the PV system and the boost converter are presented. In Section 3, an MPPT method based on P&O and FLC methodology is analyzed. The results of the experimental implementation and numerical simulations based on real climatic data are given in Section 4. Finally, Section 5 concludes the work.

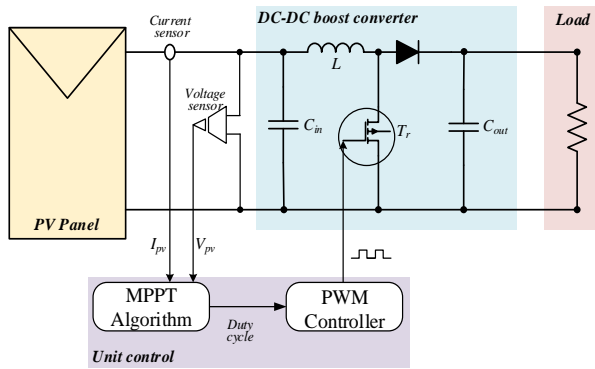


Fig. 1: PV System MPPT Algorithm.

2. PV model and characteristics

2.1. Modeling of the PV panel

Fig. 2 describes an electric model equivalent of a PV cell. It is an electronic component that, when exposed to light (photons), produces electricity thanks to the photovoltaic effect. The circuit consists of two resistors and a diode [14], [20]. R_p indicates the presence of a leakage current in the P-N junction while R_s reports the resistivity of the material and the semiconductor metal contact, the diode represents the electron hole recombination in the P-N junction.

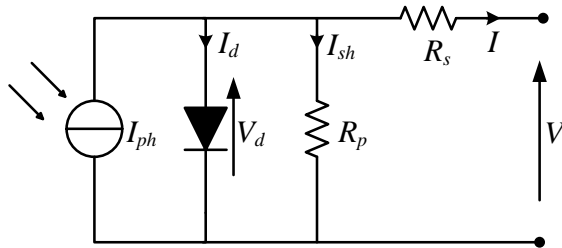


Fig. 2: Electric Model Equivalent of A PV Cell.

By applying Kirchoff's laws on the circuit of Fig. 2 above, the cell generated current is given by:

$$I = I_{ph} - I_o \left[\exp\left(\frac{V + R_s I}{nN_s V_T}\right) - 1 \right] - \frac{V + R_s I}{R_p} \quad (1)$$

where V and I are respectively voltage and current, I_o is the diode reverse saturation current, I_{ph} is the generated photocurrent, V_T is the thermal voltage ($V_T = kT/q$), k is the Boltzmann constant, n is the diode ideality factor, q is the electron charge and T is the cell's temperature (kelvin). The photocurrent is given by:

$$I_{ph} = \frac{[I_{sc} + K_i (T - T_{ref})] G}{G_{ref}} \quad (2)$$

In this previous relation, G is the radiation, G_{ref} is the nominal radiation (usually $G_{ref} = 1 \text{ kW/m}^2$) and T_{ref} is the nominal temperature in kelvin. I_o is thus given by:

$$I_o = \frac{I_{sc} + K_i \Delta T}{\exp\left[\frac{V_{oc} + K_v \Delta T}{nN_s V_T}\right] - 1} \quad (3)$$

In this paper, the parameters of the H750 PV panel under the Standard Test Condition (STC: 1 kW/m^2 and $25 \text{ }^\circ\text{C}$) are listed in Table 1.

Table 1: Electrical Parameters of the PV Module Type H750.

Parameters	Symbols	Values
Number of series cells	N_{cs}	36

Maximum Voltage	V_{mpp} (V)	17.3
Maximum Current	I_{mdd} (A)	3.17
Open-circuit voltage	V_{oc} (V)	21.6
Short-circuit current	I_{sc} (A)	4.01
Voltage coefficient	K_v (V/C $^\circ$)	-0.00123
Current coefficient	K_i (A/C $^\circ$)	3.2e-3
Maximum power	P_{mpp} (W)	60

The most important step in determining the MPP of a PV panel is to determine the current voltage and power voltage characteristics of a photovoltaic panel. The characteristic I-V and P-V curves under the STC are shown in Fig. 3.

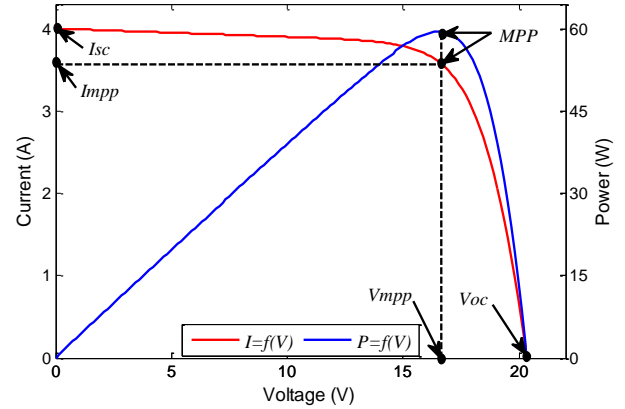


Fig. 3: I-V and P-V Characteristic of the PV Panel H750.

2.2. DC-DC boost converter modelling

Fig. 4 shows the basic configuration of a DC-DC boost converter. It operates in two states. Firstly, the switch T_r is open ($0 < t < dT$), the diode is blocked at this time and the current in the boosting inductance increases linearly. Secondly, the switch T_r is blocked ($dT < t < T$), the energy stored in the inductor is released by the diode to the output circuit [20], [23]. This leads to the following expression where V_e and V_s are respectively the input and output voltage of boost converter:

$$V_e = \left(\frac{1}{1-D} \right) V_s \quad (4)$$

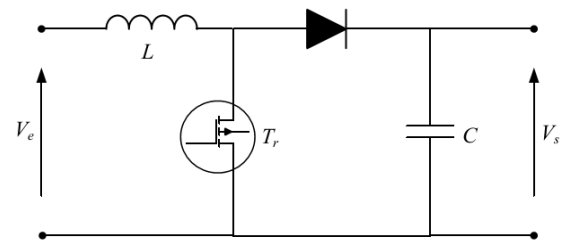


Fig. 4: Electric Model Equivalent to A Boost Converter.

The inductance L and the capacitor C of the boost converter are given by:

$$\Delta L_L = V_{e_{min}} D / f_s L \quad (5)$$

$$L = \frac{V_s (V_s - V_e)}{\Delta I_d f_s V_s} \quad (6)$$

$$C = (I_s D) / (f_s \Delta V_s) \quad (7)$$

Where $V_{e_{min}}$ is minimum input voltage, f_s is switch frequency, ΔL_L is an estimated inductor, I_s is the output current and ΔV_s is the estimated output ripple voltage [23]. The specifications of a boost converter components use in this work are listed in Table 2 below.

Table 2: Electrical Parameters of the Boost Converter

Parameters	Symbols	Values
Boost inductor	L (μH)	330
Input filter capacitor	C _{in} (μF)	330
Output filter capacitor	C _{out} (μF)	660
Switching frequency	f (kHz)	10

3. MPPT algorithms

The principle of these MPPT commands is to find the MPP by keeping a good fit between the MPP and the load to ensure the transfer of maximum available electrical power.

3.1. Perturb and observe algorithm

Fig. 5 illustrates the flowchart of the P&O MPPT command [1]-[10]. To determine the power at each moment, two sensors are needed to measure the values of voltage and current. For a disturbance of the voltage, if the power decreases, the direction of the disturbance is maintained. If not, it is inverted so that the operating point converges towards the MPP.

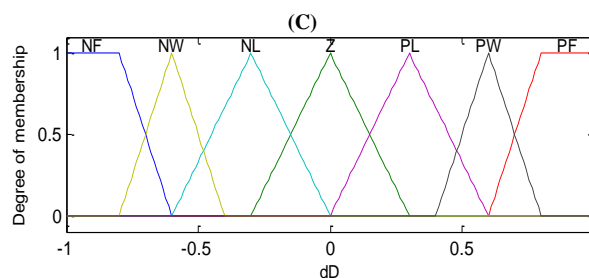
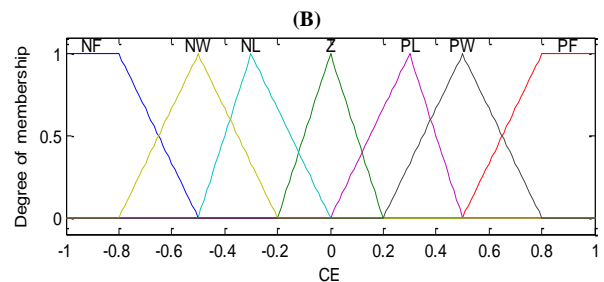
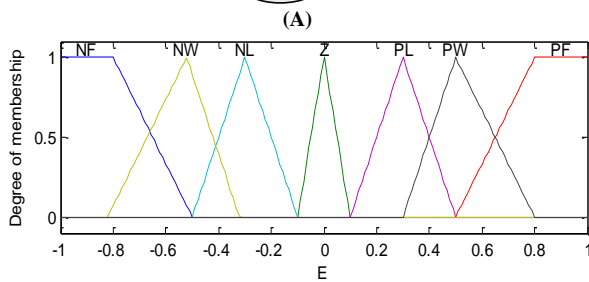
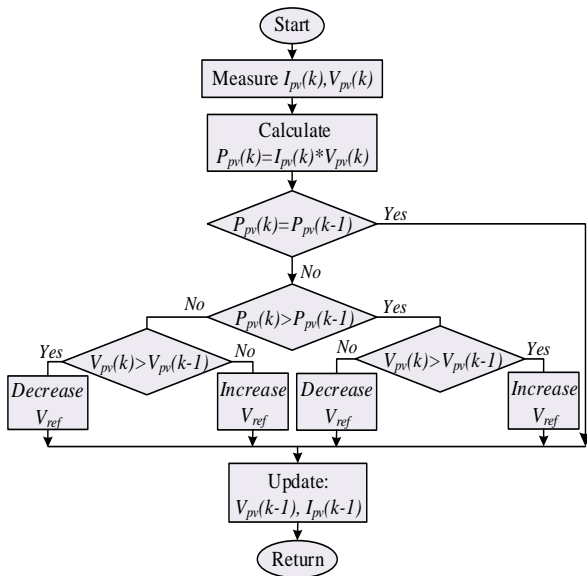


Fig. 6: Membership Functions, (A) for E (k), (B) for CE (k), and (C) for dD.

3.2.2. Inference rules

The rules between the inputs and output have to be established. Table 3 shows the fuzzy controller rule table where all the matrix

Fig. 5: Flowchart P&O Method.

3.2. Proposed fuzzy logic controller

The error E and error change CE, at times samples k are the two FLC inputs [17]-[20]. It's output is a Pulse Width Modulation (PWM) signal that controls the boost converter. The two input variables are given by:

$$E(k) = \frac{\Delta P_{pv}}{\Delta I_{pv}} = \frac{P_{pv}(k) - P_{pv}(k-1)}{I_{pv}(k) - I_{pv}(k-1)} \tag{8}$$

$$CE(k) = E(k) - E(k-1) \tag{9}$$

Where P_{pv}(k) and I_{pv}(k) are respectively the power and the current of the PV panel, E(k) indicates if the point of operation of the load at the moment k is located to the left or right of the MPP on the power characteristic curve of Fig. 3. CE(k) shows the direction of shifting of this point. The FLC contains fuzzification, basic rule and defuzzification.

3.2.1. Fuzzification

Fuzzification consists of converting the digital inputs into linguistic variables based on the degree of member functions. Fig. 6 illustrates the fuzzy sets: (A) the input error, (B) the input of the error change and (C) the output that contains seven triangular member functions.

inputs are the fuzzy sets of E (k), CE (k), and dD. Here is an example of a control rule from Table 3:
If E is Z and CE is NW, then dD is NM

Table 3: Rules of the Fuzzy System

CE	NF	NW	NL	Z	PL	PW	PF
----	----	----	----	---	----	----	----

	NF	NW	NL	Z	PL	PW	PF
E	NF	NF	NF	NW	NW	NL	Z
	NW	NF	NF	NW	NL	Z	PL
	NL	NF	NM	NM	NL	Z	PL
	Z	NM	NM	NL	Z	PL	PW
	PL	NM	NL	Z	PL	PW	PW
	PW	NL	Z	PL	PW	PM	PF
	PF	Z	PL	PW	PW	PF	PF

$$D = \left[\frac{\sum_{j=1}^n \mu(D_j) - D_j}{\sum_{j=1}^n \mu(D_j)} \right] \tag{10}$$

3.2.3. Defuzzification

The defuzzification consists of converting the output of the linguistic variable into a precise numeric variable (D):

4. Results and discussion

To assess the performance of the PV power generator, the MPPT algorithms are simulated with different scenarios.

4.1. Behaviour in the face of simultaneous variations of G and T

The PV system performance was assessed for sudden changes in climatic conditions as time is varying from 0 to 1s as shown below in Fig. 7 (A) profile 1 and (B) profile 2.

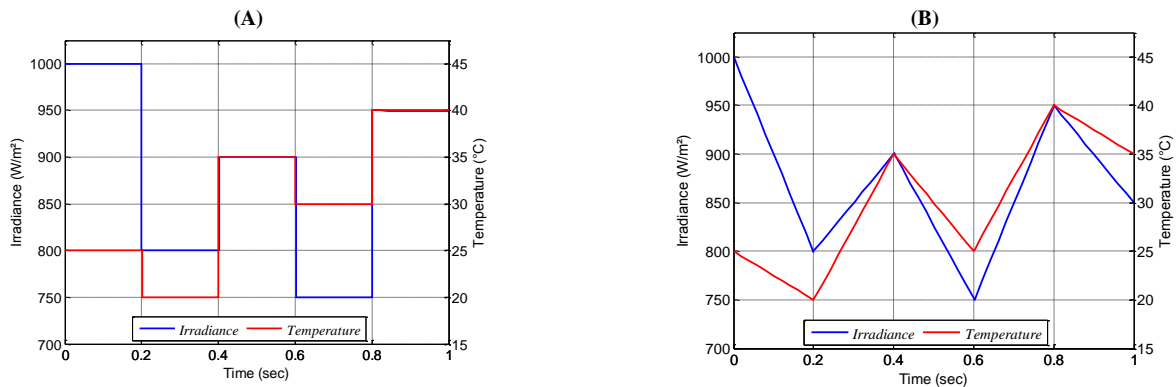


Fig. 7: Profile of Irradiance and Temperature: (A) Profile 1, (B) Profile 2.

In a first scenario, we compare by simulations, the convergence towards the MPP concerning the power of the PV system under test. This is done, by using one of the two controllers P&O and

FLC, first for the profile on the left and then on the right respectively. In Fig. 8, the left and right show the results of the simulations obtained for this first scenario.

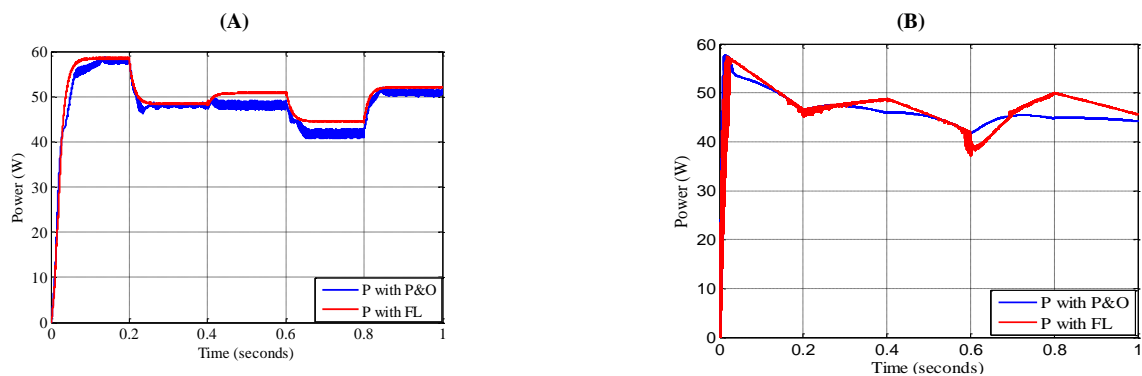


Fig. 8: Power across the Load: (A) Profile 1, (B) Profile 2.

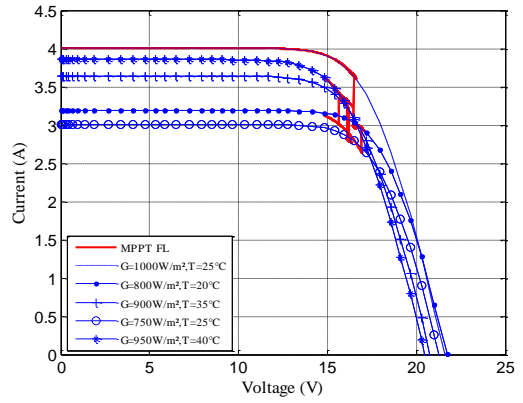
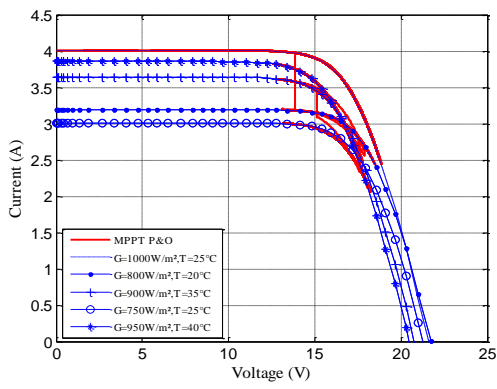
4.2. Behaviour in the vicinity of the MPP

For the second scenario, we evaluate the effectiveness of the two MPPT methods; P&O and FLC by comparing their speed of con-

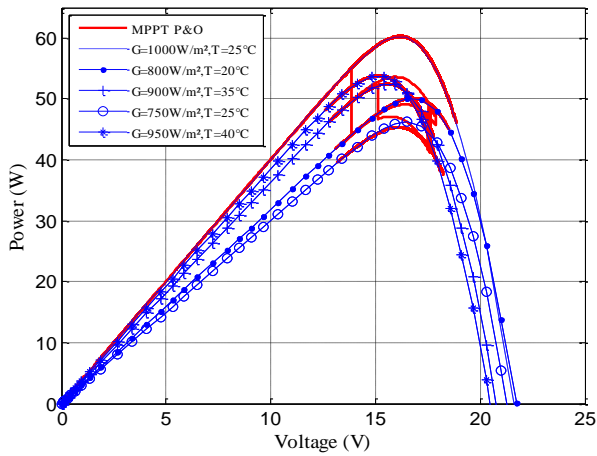
vergence and their stability with regard to the MPP at the level of the PV characteristics provided by the PV panel manufacturer H750 (refer in Table 1).

(A)

(B)



(C)



(D)

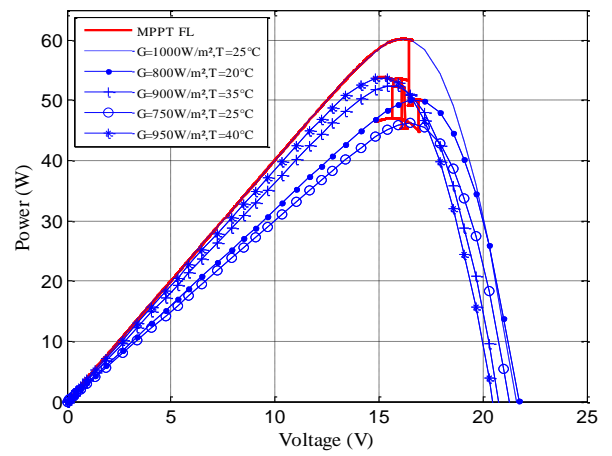
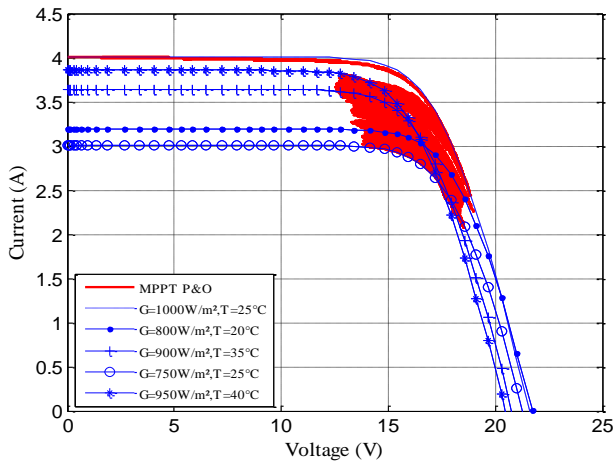
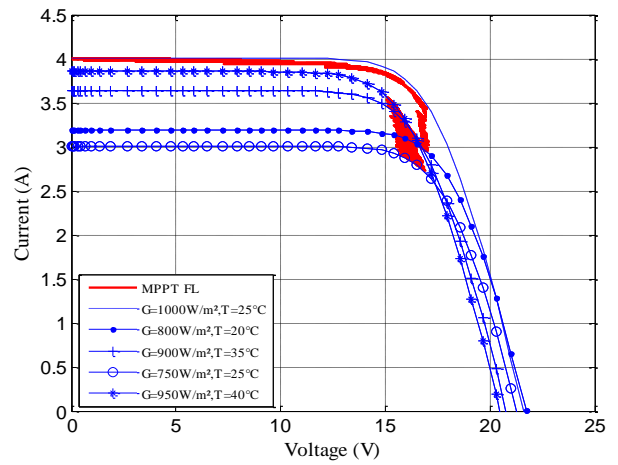


Fig. 9: Comparison of MPP Convergence of I-V and P-V Characteristics for Profile 1 Using MPPT Based on P&O (A) and (C) or FLC (B) and (D).

(A)



(B)



(C)



(D)



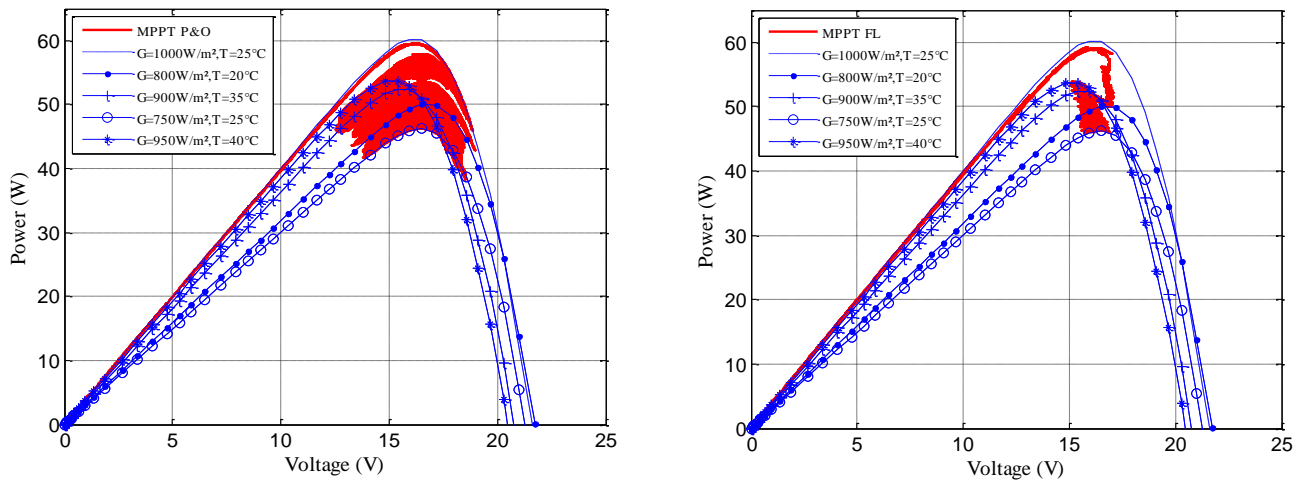


Fig. 10: Comparison of MPP Convergence of I-V and P-V Characteristics for Profile 2 Using MPPT Based on P&O (A) and (C) or FLC (B) and (D).

For this scenario, considering the above-mentioned variations and the results from Fig. 9 and Fig. 10, we deduce the behavior of the photovoltaic system for different types of MPPT (P&O and FLC) algorithms: For both algorithms, the effect of the increase in the PV produced power, caused by an increase in the illumination G and the temperature, or caused by a decrease in the temperature T and the illuminance, is noted. We can also notice that the P&O controller oscillates around the MPP, while the FLC remains fairly stable at a convergence time and a response time is faster.

Finally, for the third scenario (use a database), the two control algorithms (P&O and FLC) are simulated and tested in the MatLab/Simulink environment, under lighting and temperature modulated according to the chosen day. The simulations and comparisons are made using the measurements collected in a meteorological database of the cities of Ngaoundere and Mulhouse. In Fig. 11-(A) and Fig. 11-(B), we shows the evolution of the data recorded from 8:00 to 16:00 of the day of 17 may 2018, regarding the temperature and the lighting.

4.3. Confrontation of algorithms under real conditions

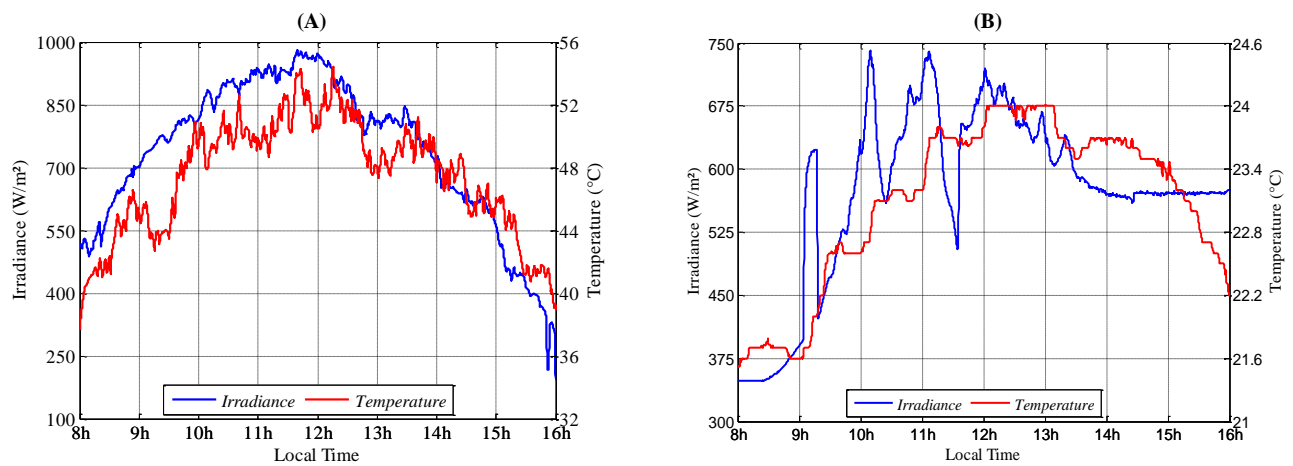


Fig. 11: Recorded Weather Data (A) LESIA Laboratory and (B) IRIMAS Laboratory.

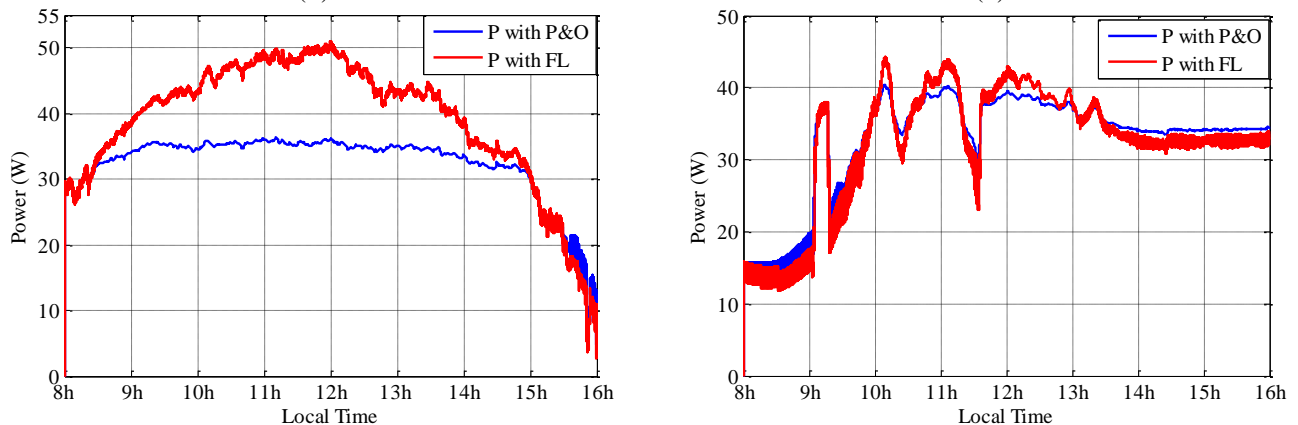


Fig. 12: Power across the Load (A) LESIA Laboratory and (B) IRIMAS Laboratory.

In this section, we examine the effects of the control provided by the two MPPT control algorithms: P&O and FLC, in the face of

variations of temperature and illumination, measured at the level of Ngaoundere and Mulhouse. These effects are illustrated by Fig.

12-(A) and Fig. 12-(B) which highlight the high efficiency, in terms of stability and response time, of the FLC with respect to the P&O based control, which thus validates the interpretations of paragraphs 4.2 and 4.4.

4.4. Performance criteria of MPPT controllers

In order to evaluate theoretically and experimentally the performances of the two types of controllers studied, our interested in this paragraph, is to compare two performance criteria of these MPPT controllers, namely:

The performance criterion η of an MPPT controller is defined by [7].

$$\eta = \frac{\int_0^t P_m(t) dt}{\int_0^t P_{max}(t) dt} \quad (11)$$

The PV system performance was assessed for sudden changes in climatic conditions as time is varying from 0 to 1s as shown below in Fig. 7 (left profile 1, right profile 2).

$$\varepsilon = \int_0^t [e(t)]^2 dt \quad (12)$$

$$e(t) = \frac{\Delta P_{pv}}{\Delta V_{pv}} \quad (13)$$

$E(t)$ is the variation of the power with respect to the variations of the output voltage of the PV panel. Based on the definitions above, for both η and ε , we find that the larger η is the lower; ε is the more efficient and faster the MPPT command will be.

In the case of our investigations, for the two MPPT algorithms discussed in this article, the table below summarizes the calculation results for the η yield and the ε criterion.

Table 4: Performance Criteria of MPPT Controllers

Performance criteria	Different MPPT algorithms	
	P&O	FL
η	97.03%	99.05%
$\varepsilon.10^6$	7.351	0.167

The comparison between these results allows us to notice that the FLC method has a better yield than that of the command P&O. Thus the criterion of the integral of the square of the error ε corresponding to the FLC method is much inferior about 50 times to the P&O command. This proves the speed of the FLC.

Table 5: Assessment of the Daily Production of Energy for Different MPPT Algorithms

Database of the cities		Different MPPT algorithms	
		P&O	FL
Ngaoundere	DMP (W)	35.32	50.76
	DAE (Wh/day)	166.69	270.07
Mulhouse	DMP (W)	30.17	31.05
	DAE (Wh/day)	150.70	160.13

5. Conclusion

In this paper, Fuzzy Logic Control (FLC) and Perturb and Observe (P&O) algorithm for MPPT of a standalone photovoltaic (PV) system have been experimentally implemented with climatic data conditions. Furthermore, results from both FLC and P&O approaches have been assessed. In order to assess their performances, numerical simulation tests under various profiles and with recorded experimental data have been carried out. The proposed fuzzy logic control based MPPT technique with triangular membership functions can track the MPP faster compared to a P&O controller. Simulation results with experimental data show the efficiency of the FLC in maintaining the stability of the MPP. Moreover, it has been proved that the proposed FLC algorithm provides superior performances against P&O results, especially regarding the speed

of tracking, the power fluctuation minimization and the efficiency in variable weather conditions.

6. Abbreviations

ANN	Artificial neural network
DAE	Daily average energy
DMP	Daily maximum power
FLC	Fuzzy logic control
FOCV	Fractional open-circuit voltage
FSCC	Fractional short-circuit current
HC	Hill climbing
INC	Incremental conductance
IRIMAS	Institute of Research in Informatics, Mathematics, Automatics and Signal
LESIA	Laboratory of energy, signal, image and automation
MPP	Maximum power point
MPPT	Maximum power point tracker
P&O	Perturb and observe
PV	Photovoltaic
PWM	Pulse width modulation
STC	Standard test condition

References

- [1] I. Houssamo, F. Locment and M. Sechilariu, "Maximum power tracking for photovoltaic power system: development and experimental comparison of two algorithms", *Renewable Energy*, Vol. 35, No.10, (2010), pp. 2381-2387, <https://doi.org/10.1016/j.renene.2010.04.006>.
- [2] A. R. Reisi, M. H. Moradi and S. Jamas, "Classification and comparison of maximum power point tracking techniques for photovoltaic system: A review", *Renewable and Sustainable Energy Reviews*, Vol. 19, (2013), pp. 433-443, <https://doi.org/10.1016/j.rser.2012.11.052>.
- [3] B. Subudhi and R. R. Pradhan, "A comparative study on maximum power point tracking techniques for photovoltaic power systems", *IEEE Transactions Sustainable Energy*, Vol. 4, No. 1, (2013) pp. 89-97, <https://doi.org/10.1109/TSTE.2012.2202294>.
- [4] A. A. Abdulrazzaq and A. H. Ali, "Evaluating the Performance and Efficiency of MPPT Algorithm for PV Systems", *International Journal of Engineering & Technology*, Vol. 7, No 4.17, (2018), pp. 66-70, <https://doi.org/10.14419/ijet.v7i4.13508>.
- [5] A. Blorfan, G. Sturtzer, D. Flieller, P. Wira and J. Mercklé, "An adaptive Control Algorithm for Maximum Power Point Tracking for Photovoltaic Energy Conversion Systems – A comparative Study", *International Review of Electrical Engineering (IREE)*, Vol 9, No. 3, (2014), pp. 559-565.
- [6] R. Verma, B. Bhargav and P. S. Varma, "Comparison of Different MPPT Algorithms for PV System", *International Journal of Engineering & Technology*, Vol. 7, No 1.8, (2018), pp. 158-163, <https://doi.org/10.14419/ijet.v7i2.31.13406>.
- [7] A. Dandoussou, M. Kamta, L. Bitjoka, P. Wira and A. Kuitché, "Comparative study of the reliability of MPPT algorithms for the crystalline silicon photovoltaic modules in variable weather conditions", *Journal of Electrical Systems and Information Technology*, Vol. 4, (2017) pp. 213-224, <https://doi.org/10.1016/j.jesit.2016.08.008>.
- [8] A. Mohapatra, B. Nayak, P. Das and K. B. Mohanty, "A review on MPPT techniques of PV system under partial shading condition", *Renewable and Sustainable Energy Reviews*, Vol. 80, (2017), pp. 854-867, <https://doi.org/10.1016/j.rser.2017.05.083>.
- [9] M. Danandeh and S. M. Mousavi, "Comparative and comprehensive review of maximum power point tracking methods for PV cells", *Renewable and Sustainable Energy Reviews*, Vol. 82, (2018), pp. 2743-2767, <https://doi.org/10.1016/j.rser.2017.10.009>.
- [10] S. Saravanan and N. Ramesh Babu, "Maximum power point tracking algorithms for photovoltaic system - A review", *Renewable and Sustainable Energy Reviews*, Vol. 57, (2016), pp. 192-204, <https://doi.org/10.1016/j.rser.2015.12.105>.
- [11] M. Jayakumar, V. Vanitha, V. Jaisuriya, M. Karthikeyan, G. Daniel and T. Vignesh, "Maximum power point tracking of a solar PV array using single stage three phase inverter", *International Journal of Engineering & Technology*, Vol. 7, No 2.31, (2018), pp. 97-100, <https://doi.org/10.14419/ijet.v7i2.31.13406>.
- [12] C. B. Yuan and L. Y. Shin, "New digital-controlled technique for battery charger with constant current and voltage control without

- current feedback”, *IEEE Transactions on Industrial Electronics*, Vol. 59, No. 3, (2012), pp. 1545-1553, <https://doi.org/10.1109/TIE.2011.2167115>.
- [13] A. E. S. A. Nafeh, F. H. Fahmy, and E. M. Abou El-Zahab, “Evaluation of a proper controller performance for maximum power point tracking of a standalone PV system”, *Solar Energy Materials and Solar Cells*, Vol. 75, No. 3, (2003), pp. 723-728, [https://doi.org/10.1016/S0927-0248\(02\)00138-1](https://doi.org/10.1016/S0927-0248(02)00138-1).
- [14] I. E. Batzelis, “Simple PV performance equations theoretically well founded on the single-diode model”, *IEEE Journal of Photovoltaics*, Vol. 7, No. 5, (2017) pp. 1400-1409, <https://doi.org/10.1109/JPHOTOV.2017.2711431>.
- [15] M. Rupesh and V. Shivalingappa, “Comparative analysis of P&O and incremental conductance method for PV system”, *International Journal of Engineering & Technology*, Vol. 7, No 3.29, (2018), pp. 519-523.
- [16] M. Gang, X. Guchao, C. Yixi and J. Rong, “Voltage stability control method of electric springs based on adaptive PI controller”, *Electrical Power and Energy Systems*, Vol. 95, (2018), pp. 202-212, <https://doi.org/10.1016/j.ijepes.2017.08.029>.
- [17] U. Yilmaz, A. Kircay and S. Borekci, “PV system fuzzy logic MPPT method and PI control as a charge controller”, *Renewable and Sustainable Energy Reviews*, Vol. 81, (2018), pp. 994-1001, <https://doi.org/10.1016/j.rser.2017.08.048>.
- [18] S. Tang, Y. Sun and Y. Chen, “An enhanced MPPT method combining fractional-order and fuzzy logic control”, *IEEE Journal of Photovoltaics*, Vol. 7, (2017), No. 2, pp. 640-650, <https://doi.org/10.1109/JPHOTOV.2017.2649600>.
- [19] L. Suganthi, S. Iniyar, Anand and A. Samuel, “Applications of fuzzy logic in renewable energy systems—A review”, *Renewable and Sustainable Energy Reviews*, Vol. 48, (2015), pp. 585-607, <https://doi.org/10.1016/j.rser.2015.04.037>.
- [20] C. B. Nzoundja Fapi, P. Wira and M. Kamta, “A Fuzzy Logic MPPT Algorithm with a PI Controller for a Standalone PV System under Variable Weather and Load Conditions”, *IEEE International Conference on Applied Smart Systems (ICASS)*, Medea, Algeria, 24-25 Nov. 2018. <https://doi.org/10.1109/ICASS.2018.8652047>.
- [21] N. Priyadarshil, A. Kr. Sharma, A. Kr. Bhoi, S. N. Ahmad, F. Azam and S. Priyam, “MatLab/simulink based fault analysis of PV grid with intelligent fuzzy logic control MPPT”, *International Journal of Engineering & Technology*, Vol. 7, No 2.12, (2018), pp. 198-204, <https://doi.org/10.14419/ijet.v7i2.12.11319>.
- [22] N. Karami, N. Moubayed and R. Outbib, “General Review and classification of different MPPT Techniques”, *Renewable and Sustainable Energy Reviews*, Vol. 68, (2017), pp. 1-18, <https://doi.org/10.1016/j.rser.2016.09.132>.
- [23] J. M. Enrique, E. Durán, M. Sidrach-de-Cardona and J. M. Andújar, “Theoretical assessment of the maximum power point tracking efficiency of photovoltaic facilities with different converter topologies”, *Solar Energy*, Vol. 81, Issue 1, (2007), pp. 31-38, <https://doi.org/10.1016/j.solener.2006.06.006>.